Modeling of Mass Transfer and Reaction Kinetics in ZnO Nanoparticle Micro-Reactor Systems for AMX and DOX Degradation

Nidhal Becheikh
Department of Chemical and Materials Engineering, Engineering College, Northern Border University, Saudi Arabia
nidhal.becheikh@nbu.edu.sa (corresponding author)

Received: 12 January 2024 | Revised: 19 February 2024 | Accepted: 28 February 2024

 DOI: https://doi.org/10.48084/etasr.6898

ABSTRACT

This study aims to model the coupled phenomena of photocatalytic reaction and mass transfer in the degradation of Amoxicillin (AMX) and Doxycycline (DOX) using Zinc oxide (ZnO) nanoparticles within microreactor systems. The objective is to gain a comprehensive understanding of the dynamic interaction between the photocatalytic degradation kinetics and the mass transfer processes to optimize the conditions for efficient antibiotic removal from contaminated water. This involves characterizing the reaction kinetics via the Langmuir-Hinshelwood model, estimating the mass transfer coefficients, and analyzing the effects of axial dispersion to ensure the accurate determination of intrinsic kinetic constants and minimize mass transfer limitations. This study used a syringe pump to ensure a consistent flow of antibiotic solution into the microreactor. The results indicate that AMX reaches adsorption equilibrium more rapidly than DOX, corresponding to its faster photocatalytic degradation kinetics and higher final conversion rate (89% for AMX, 86% for DOX). The mass transfer coefficient (k_d) was estimated using the Sherwood number, derived from three different models, with the constant Sherwood model best fitting the R1 microreactor data. An analysis of the Damköhler number (D_{aII}) indicates that high flow rates minimize mass transfer limitations in the R1 microreactor, allowing the determination of near-intrinsic kinetic constants. On the contrary, at low flow rates, kinetic constants are apparent as a result of mass-transfer limitations. The study concludes that higher flow rates (≥ 10 mL/h) in the R1 microreactor are preferable to approach intrinsic kinetics and reduce mass transfer limitations during photocatalytic degradation of antibiotics. These findings underscore the potential of ZnO-based oxidation processes in treating antibiotic-contaminated water with optimized conditions, providing a pathway for efficient and sustainable wastewater treatment.

Keywords-modeling; photocatalytic degradation; micro-reactors; kinetic constants; mass transfer limitations

I. INTRODUCTION

Water pollution causes or exacerbates the degradation of its natural qualities by altering its physical, chemical, biological, or bacteriological characteristics. This contamination comes from various anthropogenic sources, including urban, agricultural, or industrial processes [1-3]. Pollution disturbs the living conditions of fauna and flora. To solve the growing problem of pollution, strict measures are implemented to regulate water quality for human consumption [4]. These regulations are constantly adapted according to technological advances in effluent treatment processes and analysis strategies [5]. Many studies have shown the presence of various antibiotics in different environmental elements, such as wastewater from treatment plants, farms, waterways, sediments, and soils [6]. In [7], the trends and factors that influence antibiotic consumption were analyzed between 2000 and 2015 in 76 countries. According to this study, global antibiotic consumption increased by 65% between 2000 and 2015, from 21.1 to 34.8 billion Defined Daily Doses (DDD). During the same period, the rate of antibiotic consumption rose by 39%, from 11.3 to 15.7 DDD per 1,000 inhabitants per day. It was also estimated that by 2030, global antibiotic consumption will have increased by 32%, reaching approximately 55.6 billion DDD [7-9].

Traditional elimination techniques, such as adsorption, coagulation, filtration, biodegradation, or reverse osmosis, display certain limitations, either in terms of high cost or in terms of incomplete removal of pollutants. Therefore, it is essential to find suitable alternative technologies to remove toxic and biologically persistent antibiotics from wastewater [10]. Advanced Oxidation Processes (AOPs) have been developed as a highly effective alternative for converting organic materials into simple mineral products. Commonly used methods include Fenton reactions, ozonation, electrochemistry, photocatalysis, and ultrasonic. Among AOPs, heterogeneous photocatalysis is the most promising solution for environmental decontamination due to its nonselective nature,

high efficiency in removing various pollutants from wastewater, including antibiotics, and its ability to effectively reduce toxicity [11-13].

AOPs rely on in situ production of highly reactive and oxidizing radical species, like peroxyl organic radicals, hydroxyl radicals, molecular singlet oxygen, or superoxide anion radicals [14]. These species interact with organic pollutants and lead to their fragmentation. The hydroxyl radical is particularly reactive and relatively non-selective, has a powerful oxidation capacity, and is the second most reactive species after the fluorine atom, with a redox potential of 2.8 eV and a marked electrophilic character [15]. In this wide range of techniques, two main categories can be distinguished: homogeneous and heterogeneous phase processes. These two classes can also be subdivided into two subcategories depending on whether or not energy is used to enhance the production of oxidative radical species and thus water treatment. Heterogeneous photocatalysis has been applied to the degradation of various pollutants, namely pesticides, insecticides, and dyes, which can be completely oxidized to CO_2 and H_2O [16-17]. Photocatalytic reactions involve the participation of one or more chemical compounds, a photocatalyst, and a photon flux. Numerous physicochemical parameters, such as the concentration of dissolved oxygen, temperature, pH, crystal structure, and specific surface, have also been identified to influence photocatalytic kinetics. Extensive studies have been conducted on these physicochemical parameters to better understand their impact on the kinetics of photocatalytic reactions [18-19].

Zinc oxide (ZnO) is one of the semiconductor materials widely employed in photocatalytic applications because of its various advantages, such as non-toxicity, ecological properties, natural abundance, low cost, photochemical stability, high surface area, and straightforward preparation techniques. However, the rapid recombination of photoexcited e^-/h^+ pairs, the high bandgap (~3.3 eV), and the required excitation energy of 60 meV are inherent obstacles to achieving higher photocatalytic activity from ZnO nanostructures [20-21]. The use of ZnO for photocatalytic degradation of antibiotics has been investigated in several studies, encompassing a variety of ZnO forms, including nanoparticles, microparticles, and multiple composites [22-24]. In [25-26], it was shown that ZnO effectively degrades antibiotic pollutants, like tetracycline hydrochloride (TCH), ciprofloxacin (CIP), and sulfamethoxazole (SMX). The efficiency of ZnO in the photocatalytic degradation process is affected by factors, such as its structural form, environmental reaction conditions (including pH and flow rate), and interaction with other photocatalytic materials. The degradation mechanism is primarily facilitated by reactive species, namely superoxide radicals (O_2^-) and holes (h^+). Typically, the degradation kinetics of antibiotics via ZnO adhere to pseudo-first-order kinetics. The stability and recyclability of ZnO-based photocatalysts are commendable, underscoring their potential for sustainable use in wastewater treatment [27-28].

However, the modeling of mass transfer and photocatalytic reactions has been investigated. Several studies have proposed mathematical and numerical models to understand the kinetics and parameters that influence the reaction [29-30]. These models consider factors, such as Langmuir-Hinshelwood (LH) kinetics, mass transfer theory, and the relative contributions of mass transport and intrinsic kinetics to the apparent reaction rate [1, 31]. Despite the significant number of proposed models that allow coupling photocatalytic reactions and mass transfer, the extrapolation of these models is generally limited by a set of considerations, involving the configuration of the reactor or microreactor, the type and concentration of the pollutant, the catalyst, and the hydrodynamic conditions. This study falls within this theme and aims to model the photocatalytic degradation of two antibiotic pollutants, Amoxicillin (AMX) and Doxycycline (DOX), by determining the kinetic constants k and adsorption constants K of the LH model.

II. EXPERIMENTAL METHOD

A. Pollutants: AMX and DOX

The pollutants tested in the study belong to two distinct classes of antibiotics, which are differentiated by their unique molecular structures. These classes are beta-lactams and tetracyclines. The specific pollutants examined in this case are AMX and DOX, and Table I depicts their characteristics.

TABLE I. PHYSICOCHEMICAL PROPERTIES OF PHARMACEUTICAL PRODUCTS.

Antibiotic	Class	Formula	Molecular weight (g/mol)	λ_max (nm)
Amoxicillin	Beta-lactams	$C_{16}H_{19}N_3O_5S$	365.4	230 and 270
Doxycycline	Tetracycline	$C_{22}H_{24}N_2O_8$	444.4	274 and 346

A Thermo Scientific Evolution 300 model spectrophotometer, which offers a spectral range of 190 to 1100 nm, was put into service. Its precision is ±1 nm, its reproducibility is 0.1 nm, and its spectrum scanning speed is 240 nm/min. A 10 mm quartz cuvette was used for the measurement. Two lamps were employed: a mercury lamp to serve as the main reference standard to validate and calibrate the instrument, and a xenon lamp, which was activated only during measurements. Blanks were performed utilizing ultrapure water in a quartz cuvette identical to the one used for the samples. Residual concentrations were determined by interpolation deploying calibration curves or spectra $A = f(\lambda)$. AMX and DOX antibiotics were utilized for photocatalytic degradation, which absorb in UV-visible at wavelengths of 230 and 270 nm and 275 and 347 nm, as observed in Figures 1 and 2, respectively. These wavelengths were implemented to monitor the degradation kinetics by UV-visible spectroscopy.

B. Photocatalytic Degradation

The experimental setup consists of a microreactor where the photocatalytic reaction occurs, a UV lamp that irradiates the microchannel, and a syringe pump that ensures the flow of an aqueous solution containing the pollutant (AMX or DOX) at a known concentration (C = 10 mg/L) into the microreactor. The microreactors had ZnO nanoparticles dispersed in a water/ethanol solution (30% ethanol). The surface of the microchannel was covered by the water/ethanol solution containing the ZnO particles. The microreactor was then placed in an oven at 60°C for one hour to ensure drying. Figure 3

exhibits the experimental assembly applied. The microreactors were manufactured in polymer with different geometries (width, depth, and length) using a 3D printer to study the photocatalytic activity as a function of the microchannel characteristics. Table II lists the different characteristic dimensions of the microreactors.

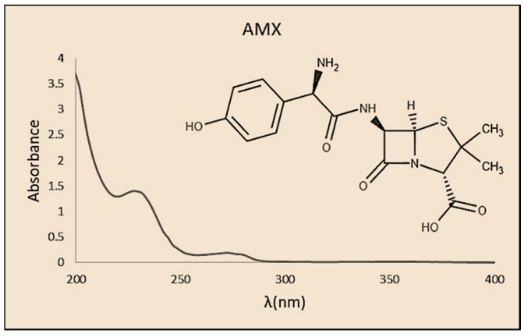

Fig. 1. UV absorption spectrum of AMX at 10 mg/L.

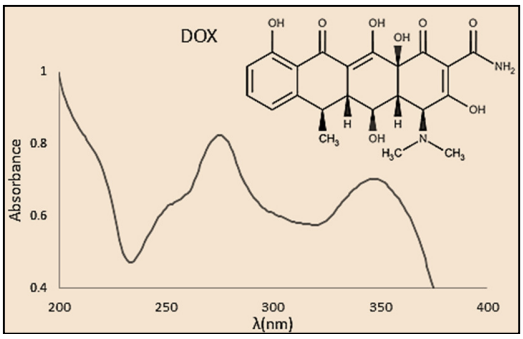

Fig. 2. UV absorption spectrum of DOX at 10 mg/L.

TABLE II. DIFFERENT DIMENSIONS OF MICROREACTORS

	Width w (mm)	Depth d (mm)	Length L (mm)	Volume V (mm³)
R1	1	2	120	240
R2	3	2	120	720
R3	2	3	120	720

III. RESULTS AND DISCUSSION

A. Results of Photocatalytic Degradation

The syringe pump, demonstrated in Figure 3, was employed to inject a solution containing an initial antibiotic concentration (Ce) of 10 mg/L into the microreactor. Once the flow rate was set, the syringe pump ensured regular injection of the solution. At regular time intervals, samples were taken from the treated solution and their concentration was measured utilizing UV-visible spectroscopy. These measurements allow the determination of the exit concentration (Cso) of the antibiotic at a given time, which corresponds to the experimental time required to obtain a representative sample. The irradiation of the ZnO photocatalyst was initiated after the establishment of the adsorption-desorption equilibrium, which occurs at 52 minutes. Figure 4 portrays the degradation of AMX and DOX antibiotics on the ZnO photocatalyst before and after the initiation of irradiation.

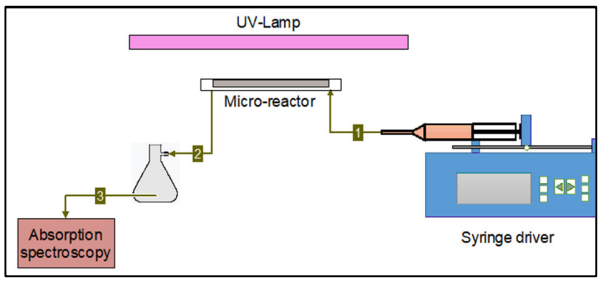

Fig. 3. Experimental setup for photocatalytic degradation in microreactor.

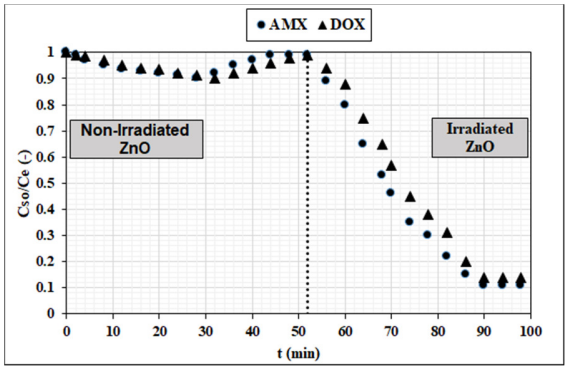

Fig. 4. Evolution of Cso/Ce in R1 at a flow rate of 2.5 mL/h, in the absence and with irradiation. Ce = 10 mg/L.

At a fixed flow rate and identical initial concentrations, the times required to reach the adsorption equilibrium states differ between the various antibiotics. In this case, the adsorption equilibrium states of AMX are established after 40 minutes, while the adsorption-desorption equilibrium of DOX, as well as the mixture of antibiotics, requires 52 minutes. This suggests that the adsorption processes of each antibiotic have different rates, leading to different equilibrium times. Irradiation instantly causes a drop in AMX and DOX concentrations, achieving final conversion rates of 89% and 86%, respectively. It is important to note that the kinetics of photocatalytic degradation for AMX and DOX are different. Moreover, the maximum conversion of AMX is notably significant. This behavior is similar to the concentration fluctuations observed during the adsorption-desorption processes of antibiotics. The processes of adsorption, desorption, and photocatalytic reaction proceed concurrently. Because of the faster adsorption kinetics of AMX, the molecules adsorbed on the catalyst surface rapidly oxidize and decompose into byproducts.

B. Modeling of the Photocatalytic Reaction

Using this axial dispersion plug flow reactor model, it is possible to account for the effects of axial dispersion in the reactor, which allows for a more accurate representation of reality compared to the simplified model of the ideal plug flow reactor. This is particularly important when significant concentration variations occur in the reactor due to the effects of diffusion, convection, or non-ideality. The balance equation in a plug flow reactor with axial dispersion is written as follows:

$$D_A \frac{d^2C}{dx^2} = U\frac{dC}{dx} + r \quad (1)$$

Considering the concentration variation between the reaction medium and the catalytic surface, the LH model can be applied to describe the apparent rate of the photocatalytic reaction.

$$r_a = r_D = K_D a\,(C_b - C_s) = k_r \frac{KC_s}{1+KC_s} \quad (2)$$

According to this model, this rate is in balance with the mass transfer rate, denoted as r_D. This equation expresses the specific relationship and allows for the calculation of the surface concentration C_s, the conversion rate, and the mass transfer coefficient. In this equation, r_a is the apparent rate of the photocatalytic reaction (mmol/L/s), r_D is the mass transfer rate (mmol/L/s), K_D is the mass transfer coefficient (m/s), a is the specific surface area of the catalytic surface (mm^2/mm^3), C_s is the surface concentration on the catalytic surface (mmol/L), C_b is the concentration in the reaction phase (mmol/L), and k_r is the rate constant of the chemical reaction (mmol/L/s). Trough this equation, it is possible to determine C_s from the concentration in the reaction phase C and other parameters. Furthermore, the conversion rate can be calculated based on C_s and the initial concentration of the reactive species.

$$X = 1 - exp\left(\frac{L}{2}\left(\frac{U}{D_A} - \sqrt{\left(\frac{U}{D_A}\right)^2 + \frac{4}{D_A}\frac{k_r K k_d}{k_d(1+KC_S)+k_r K}}\right)\right) \quad (3)$$

The mass transfer coefficient k_d can be estimated from the Sherwood number using:

$$Sh = \frac{k_d\, d_h}{D_m} \quad (4)$$

Table III illustrates common models utilized to estimate the Sherwood number in microreactors.

TABLE III. MODELS USED TO ESTIMATE THE SHERWOOD NUMBER IN MICRO-REACTORS

Model	Equation
Constant Sherwood Model	$Sh = 3.66$
Graetz-Lévêque (GL)	$Sh = 1.86\left(\frac{d_h}{L}\right)^{0,33} R_e^{0,33} S_C^{0,33}$
Ranz-Lenvenspiel (RL)	$Sh = 2 + 1.8\, R_e^{0,33} S_C^{0,33}$

In this table, Sh denotes the Sherwood number (dimensionless), d_h is the hydraulic diameter (m), which is equal to 4(w×d)/(2(w+d)), L is the characteristic length (m), R_e is the Reynolds number (dimensionless), and S_c is the Schmidt number (dimensionless). Equation 3 was solved by fitting the experimental results engaging an Excel solver. This technique allowed the estimation of the kinetic and adsorption constants. Moreover, the determination of the mass transfer constant was carried out by testing the three models proposed in Table III. Kinetic constant determination was performed by fitting the described models to the experimental results for the micro-reactor R1 as detected in Figure 5. The findings of the conversion rates in the microreactor R1 are accurately modeled by the constant Sherwood model. However, this conclusion cannot be generalized to other microreactors with different hydraulic diameters. To verify the effect of changes in hydraulic diameter on the mass transfer coefficient, a comparison of the experimental conversion rate results in microreactors R2 and R3 and the mass transfer models was carried out, as displayed in Figures 6 and 7.

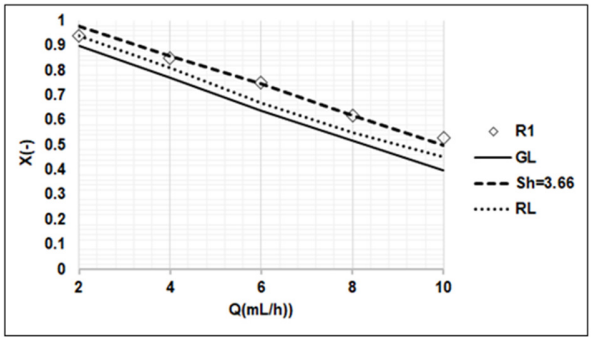

Fig. 5. Experimental and theoretical conversion rates calculated by the models of S_h=3.66, GL and RL as a function of flow rate in R1, C_e = 10 mg/L, I = 1.5 mW/cm², K = 75.10^{-4} L/mmol and k_r=50 mmol/L.s.

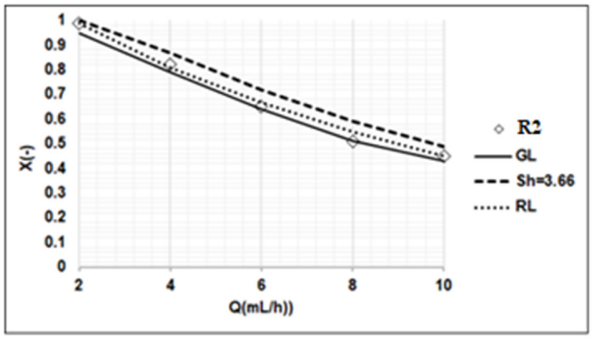

Fig. 6. Experimental and theoretical conversion rates calculated by the models of S_h=3.66, GL, and RL as a function of flow rate in R2, C_e = 10 mg/L, I = 1.5 mW/cm², K = 75.10^{-4} L/mmol, and k_r=50 mmol/L.s.

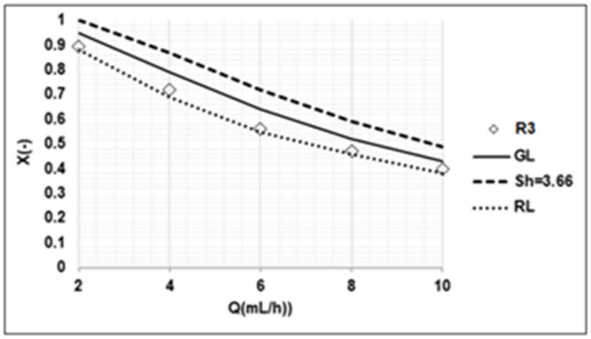

Fig. 7. Experimental and theoretical conversion rates calculated by the models of S_h=3.66, GL and RL as a function of flow rate in R3, C_e = 10 mg/L, I = 1.5 mW/cm², K = 75.10^{-4} L/mmol, and k_r=50 mmol/L.s.

The conversion rate outcomes in the microreactors R2 and R3 were accurately modeled as a function of the flow rates by the RL model. It is interesting to note that the model allowed the linking of mass transfer to the flow regime via the Reynolds number. Indeed, at different flow rates, it was observed that the model with S_h = 3.66 does not accurately reproduce the experimental conversion rates.

C. Influence of Mass Transfer

To ensure that the kinetic data measured for the degradation of AMX and DOX accurately reflect the intrinsic kinetics, it is necessary to analyze the mass transfer limitations. In the context of microchannel reactors, if the heterogeneous

Damköhler number (D_{aII}) is below 0.1, the error in the measured rate constants is kept below 3%. This condition allows for the assumption that these constants are a valid representation of the intrinsic kinetics of the photocatalytic degradation of AMX and DOX.

$$Da_{II} = \frac{k_r}{a.k_{d.}/K + a.k_d.C_b} \quad (8)$$

Figure 8 demonstrates the values of the Damköhler number D_{aII} versus the flow rate for different microreactors. Analysis of the variation of the Damköhler number as a function of flow rate indicates that the photocatalytic degradation in microreactor R1 exhibits a slight limitation by mass transfer and that the experimentally determined kinetic constants at high volumetric flows are close to the intrinsic constants. On the other hand, for low flow rates, kinetic constants are considered apparent. Similarly, for microreactors R2 and R3, the photocatalytic degradation process is limited by mass transfer. In conclusion, using the R1 at high flow will allow overcoming the limitation of mass transfer.

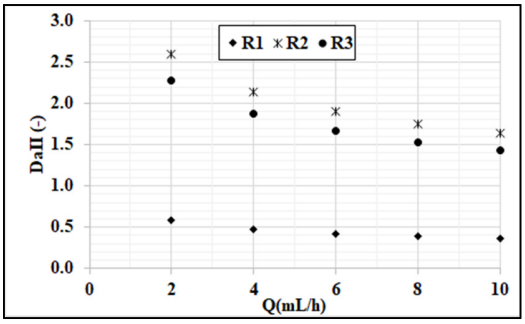

Fig. 8. Damköhler number D_{aII} for different micro-reactors vs flow rate.

IV. CONCLUSION

This study models the mass transfer and reaction kinetics of ZnO nanoparticle microreactor systems, focusing on the degradation of AMX and DOX antibiotics. The former provides a deep understanding of the dynamic interaction between photocatalytic degradation kinetics and mass transfer processes, which is vital for optimizing antibiotic removal from contaminated water. Three microreactors were manufactured in polymer with different geometries using a 3D printer to study the photocatalytic activity as a function of the microchannel characteristics. The results reveal distinct adsorption and degradation behavior for AMX and DOX, with AMX reaching adsorption equilibrium more swiftly and achieving a higher conversion rate of 89%, compared to the conversion rate of 86% for DOX. Employing this axial dispersion plug flow reactor model, it is possible to account for the effects of axial dispersion in the reactor, which allows for a more accurate representation of reality compared to the simplified model of the ideal plug flow reactor. This is particularly important when significant concentration variations occur in the reactor due to the effects of diffusion, convection, or non-ideality. The determination of the conversion rate was solved by fitting the experimental results deploying an Excel solver. This technique allowed for the estimation of the kinetic and adsorption constants. Moreover, the determination of the mass transfer constant was carried out by testing three different Sherwood models. The conversion rate results in the microreactor R1 are accurately modeled by the constant Sherwood model. However, the R2 and R3 microreactors were accurately modeled using the RL model. The analysis of the variation of the Damköhler number discloses that the photocatalytic degradation in the R1 microreactor exhibits a minor limitation by mass transfer and that the experimentally determined kinetic constants at high volumetric flows are close to the intrinsic constants. On the other hand, for low flow rates, the determined kinetic constants are considered apparent. For microreactors R2 and R3, the photocatalytic degradation process is limited by mass transfer. In conclusion, utilizing the R1 microreactor at high flow rates (≥10mL/h) enables overcoming the mass transfer limitation.

V. ACKNOWLEDGMENTS

The authors extend their appreciation to the Deanship of Scientific Research at Northern Border University, Arar, KSA for funding this research work through project number NBU-FFR-2024- 2933-01.

REFERENCES

[1] Md. G. Uddin, S. Nash, and A. I. Olbert, "A review of water quality index models and their use for assessing surface water quality," *Ecological Indicators*, vol. 122, Mar. 2021, Art. no. 107218, https://doi.org/10.1016/j.ecolind.2020.107218.

[2] N. Akhtar, M. I. Syakir Ishak, S. A. Bhawani, and K. Umar, "Various Natural and Anthropogenic Factors Responsible for Water Quality Degradation: A Review," *Water*, vol. 13, no. 19, Jan. 2021, Art. no. 2660, https://doi.org/10.3390/w13192660.

[3] F. Zenati, A. Djellali, and D. Sarker, "Wastewater Assessment and Biochemical Oxygen Demand Value Prediction from Mining Operations: A Case Study," *Engineering, Technology & Applied Science Research*, vol. 13, no. 3, pp. 10754–10758, Jun. 2023, https://doi.org/10.48084/etasr.5721.

[4] D. S. Malik, A. K. Sharma, A. K. Sharma, R. Thakur, and M. Sharma, "A review on impact of water pollution on freshwater fish species and their aquatic environment," in *Advances in Environmental Pollution Management: Wastewater Impacts and Treatment Technologies*, Haridwar, India: Agro Environ Media, 2020, pp. 10–28.

[5] R. Alduina, "Antibiotics and Environment," *Antibiotics*, vol. 9, no. 4, Apr. 2020, Art. no. 202, https://doi.org/10.3390/antibiotics9040202.

[6] M. Bilal, S. Mehmood, T. Rasheed, and H. M. N. Iqbal, "Antibiotics traces in the aquatic environment: persistence and adverse environmental impact," *Current Opinion in Environmental Science & Health*, vol. 13, pp. 68–74, Feb. 2020, https://doi.org/10.1016/j.coesh.2019.11.005.

[7] E. Y. Klein *et al.*, "Global increase and geographic convergence in antibiotic consumption between 2000 and 2015," *Proceedings of the National Academy of Sciences*, vol. 115, no. 15, pp. E3463–E3470, Apr. 2018, https://doi.org/10.1073/pnas.1717295115.

[8] A. Z. Al Meslamani, "Antibiotic resistance in low- and middle-income countries: current practices and its global implications," *Expert Review of Anti-infective Therapy*, vol. 21, no. 12, pp. 1281–1286, Dec. 2023, https://doi.org/10.1080/14787210.2023.2268835.

[9] P. Kovalakova, L. Cizmas, T. J. McDonald, B. Marsalek, M. Feng, and V. K. Sharma, "Occurrence and toxicity of antibiotics in the aquatic environment: A review," *Chemosphere*, vol. 251, Jul. 2020, Art. no. 126351, https://doi.org/10.1016/j.chemosphere.2020.126351.

[10] R. N. Abbas and A. S. Abbas, "The Taguchi Approach in Studying and Optimizing the Electro-Fenton Oxidation to Reduce Organic Contaminants in Refinery Wastewater Using Novel Electrodes," *Engineering, Technology & Applied Science Research*, vol. 12, no. 4, pp. 8928–8935, Aug. 2022, https://doi.org/10.48084/etasr.5091.

[11] J. Wang and S. Wang, "Reactive species in advanced oxidation processes: Formation, identification and reaction mechanism," *Chemical Engineering Journal*, vol. 401, Dec. 2020, Art. no. 126158, https://doi.org/10.1016/j.cej.2020.126158.

[12] J. Wang and R. Zhuan, "Degradation of antibiotics by advanced oxidation processes: An overview," *Science of The Total Environment*, vol. 701, Jan. 2020, Art. no. 135023, https://doi.org/10.1016/j.scitotenv. 2019.135023.

[13] S. Li *et al.*, "Antibiotics degradation by advanced oxidation process (AOPs): Recent advances in ecotoxicity and antibiotic-resistance genes induction of degradation products," *Chemosphere*, vol. 311, Jan. 2023, Art. no. 136977, https://doi.org/10.1016/j.chemosphere.2022.136977.

[14] P. Krystynik, "Advanced Oxidation Processes (AOPs) – Utilization of Hydroxyl Radical and Singlet Oxygen," in *Reactive Oxygen Species*, IntechOpen, 2021.

[15] C. Amor, J. R. Fernandes, M. S. Lucas, and J. A. Peres, "Hydroxyl and sulfate radical advanced oxidation processes: Application to an agro-industrial wastewater," *Environmental Technology & Innovation*, vol. 21, Feb. 2021, Art. no. 101183, https://doi.org/10.1016/j.eti.2020. 101183.

[16] A. G. Akerdi and S. H. Bahrami, "Application of heterogeneous nano-semiconductors for photocatalytic advanced oxidation of organic compounds: A review," *Journal of Environmental Chemical Engineering*, vol. 7, no. 5, Oct. 2019, Art. no. 103283, https://doi.org/ 10.1016/j.jece.2019.103283.

[17] K. Bano, S. Kaushal, and P. P. Singh, "A review on photocatalytic degradation of hazardous pesticides using heterojunctions," *Polyhedron*, vol. 209, Nov. 2021, Art. no. 115465, https://doi.org/10.1016/j.poly. 2021.115465.

[18] S. Bagheri, A. TermehYousefi, and T.-O. Do, "Photocatalytic pathway toward degradation of environmental pharmaceutical pollutants: structure, kinetics and mechanism approach," *Catalysis Science & Technology*, vol. 7, no. 20, pp. 4548–4569, Oct. 2017, https://doi.org/ 10.1039/C7CY00468K.

[19] I. Khan, K. Saeed, N. Ali, I. Khan, B. Zhang, and M. Sadiq, "Heterogeneous photodegradation of industrial dyes: An insight to different mechanisms and rate affecting parameters," *Journal of Environmental Chemical Engineering*, vol. 8, no. 5, Oct. 2020, Art. no. 104364, https://doi.org/10.1016/j.jece.2020.104364.

[20] A. Mir, N. Becheikh, L. Khezami, M. Bououdina, and A. Ouderni, "Synthesis, Characterization, and Study of the Photocatalytic Activity upon Polymeric-Surface Modification of ZnO Nanoparticles," *Engineering, Technology & Applied Science Research*, vol. 13, no. 6, pp. 12047–12053, Dec. 2023, https://doi.org/10.48084/etasr.6373.

[21] F. H. Abdullah, N. H. H. A. Bakar, and M. A. Bakar, "Current advancements on the fabrication, modification, and industrial application of zinc oxide as photocatalyst in the removal of organic and inorganic contaminants in aquatic systems," *Journal of Hazardous Materials*, vol. 424, Feb. 2022, Art. no. 127416, https://doi.org/10.1016/j.jhazmat. 2021.127416.

[22] T. H. Nguyen, T. A. N. Cong, and A.-T. Vu, "Synthesis of Carnation-Like ZnO for Photocatalytic Degradation of Antibiotics, Including Tetracycline Hydrochloride," *Environmental Engineering Science*, vol. 40, no. 8, pp. 329–339, Aug. 2023, https://doi.org/10.1089/ees.2023. 0034.

[23] S. Zeinali Heris, M. Etemadi, S. B. Mousavi, M. Mohammadpourfard, and B. Ramavandi, "Preparation and characterizations of TiO2/ZnO nanohybrid and its application in photocatalytic degradation of tetracycline in wastewater," *Journal of Photochemistry and Photobiology A: Chemistry*, vol. 443, Sep. 2023, Art. no. 114893, https://doi.org/10.1016/j.jphotochem.2023.114893.

[24] M. R. da Silva, D. L. Cunha, and E. M. Saggioro, "Insight into antibiotic degradation through photocatalysis processes: Photocatalysts semiconductors, transformation products and influencing factors." Research Square, Jun. 06, 2023, https://doi.org/10.21203/rs.3.rs-2865739/v1.

[25] X. Yu *et al.*, "Preparation of ZnO/Cu2O Composite Particles and Its Degradation of Ciprofloxacin: Analysis of Degradation Performance and Active Species," *Integrated Ferroelectrics*, vol. 236, no. 1, pp. 96–108, Jul. 2023, https://doi.org/10.1080/10584587.2023.2194831.

[26] N. Roy, K. Kannabiran, and A. Mukherjee, "Integrated adsorption and photocatalytic degradation based removal of ciprofloxacin and sulfamethoxazole antibiotics using Fc@rGO-ZnO nanocomposite in aqueous systems," *Chemosphere*, vol. 333, Aug. 2023, Art. no. 138912, https://doi.org/10.1016/j.chemosphere.2023.138912.

[27] R. K. Dharman, A. Mariappan, and T. H. Oh, "Accelerated photocatalytic degradation of sulfonamide antibiotic pollutant using oxygen vacancy in metal-organic framework ZIF-8/Ag3PO4 heterostructure," *Surfaces and Interfaces*, vol. 39, Jul. 2023, Art. no. 102998, https://doi.org/10.1016/j.surfin.2023.102998.

[28] M. Sharma *et al.*, "Photocatalytic degradation of four emerging antibiotic contaminants and toxicity assessment in wastewater: A comprehensive study," *Environmental Research*, vol. 231, Aug. 2023, Art. no. 116132, https://doi.org/10.1016/j.envres.2023.116132.

[29] J. C. G. da Silva, J. L. F. Alves, G. D. Mumbach, and M. Di Domenico, "Photocatalytic degradation of ethylene in tubular microreactor coated with thin-film of TiO2: Mathematical modeling with experimental validation and geometry analysis using computational fluid dynamics simulations," *Chemical Engineering Research and Design*, vol. 196, pp. 101–117, Aug. 2023, https://doi.org/10.1016/j.cherd.2023.06.036.

[30] R. Mondal, "Micro-segregated two-dimensional fluid and mass transport modelling in unsteady rotating annular photocatalytic reactor," *Results in Engineering*, vol. 16, Dec. 2022, Art. no. 100752, https://doi.org/10.1016/j.rineng.2022.100752.

[31] N. A. B. Timmerhuis, J. A. Wood, and R. G. H. Lammertink, "Connecting experimental degradation kinetics to theoretical models for photocatalytic reactors: The influence of mass transport limitations," *Chemical Engineering Science*, vol. 245, Dec. 2021, Art. no. 116835, https://doi.org/10.1016/j.ces.2021.116835.